Scale-selective Time Integration for Long-Wave Linear Acoustics

Stefan Vater, Rupert Klein and Omar M. Knio

Abstract In this note, we present a new method for the numerical integration of one dimensional linear acoustics with long time steps. It is based on a scale-wise decomposition of the data using standard multigrid ideas and a scale-dependent blending of basic time integrators with different principal features. This enables us to accurately compute balanced solutions with slowly varying short-wave source terms. At the same time, the method effectively filters freely propagating compressible short-wave modes. The selection of the basic time integrators is guided by their discrete-dispersion relation. Furthermore, the ability of the schemes to reproduce balanced solutions is shortly investigated. The method is meant to be used in semi-implicit finite volume methods for weakly compressible flows.

Key words: linear acoustics, implicit time discretization, large time steps, balanced modes, multiscale time integration
MSC2010: 35L05, 65M06, 86-08, 86A10

1 Introduction

General circulation models (GCMs) currently used for planetary flow simulations, are based on the Hydrostatic Primitive Equations. This approximation of the full compressible flow equations suppresses vertically propagating sound waves, but it still admits horizontally traveling long wave acoustics, so called "Lamb waves". These and other effects of compressibility are increasingly considered to be non-negligible for planetary-scale dynamics [1, 6]. On the other hand, modern high-

Stefan Vater, Rupert Klein
Institut für Mathematik, Freie Universität Berlin, Berlin, Germany, e-mail: stefan.vater@math.fu-berlin.de, rupert.klein@math.fu-berlin.de

Omar M. Knio
Dept. of Mechanical Eng., Johns Hopkins University, Baltimore, USA, e-mail: knio@jhu.edu

Published in: **Finite Volumes for Complex Applications VI – Problems & Perspectives** (2011), Fořt, J.; Fürst, J.; Halama, J.; Herbin, R.; Hubert, F. (eds.), Springer Proceedings in Mathematics 4, pp. 771–779, DOI: 10.1007/978-3-642-20671-9_81.
The original publication is available at http://www.springerlink.com

performance computing hardware is beginning to allow the usage of grids with horizontal spacings of merely a few kilometers in such applications (see e.g. [5]). This development introduces considerable numerical difficulties. For explicit time integration schemes, the propagation of sound perturbations introduced by compressibility require very small time steps $\Delta t \sim \Delta x/c$, where Δx is the typical computational grid size, and c a characteristic sound speed. Alternatively, the application of implicit time discretizations solves the problem of the severe time step restriction, but it introduces potentially undesirable numerical dispersion: Most – if not all – existing implicit schemes slow down modes with high wave numbers. Furthermore, there are quite popular schemes, such as the implicit trapezoidal scheme, which preserve the amplitude for all wave numbers. Being a desirable feature at the first glance, it is a potential source of nonlinear instabilities in practice.

In the present work, a new discretization of the linearized acoustic equations is introduced, which overcomes some of the disadvantages of standard implicit discretizations with respect to the representation of compressibility. This means that the scheme should represent the "slaved" dynamics of short-wave solution components induced by slow forcing or arising in the form of high-order corrections to long-wave modes with second-order accuracy. Furthermore, it should eliminate freely propagating compressible short-wave modes that are under-resolved in time, while minimizing dispersion for resolved modes. Here, we describe first successful steps to achieve our goals.

Governing equations. The equations for one dimensional linear acoustics are given by the system

$$\begin{aligned} m_t + p_x &= 0 \\ p_t + c^2 m_x &= q(t, \tfrac{x}{\varepsilon}) \ , \end{aligned} \tag{1}$$

where $p = p(t,x)$ and $m = m(t,x)$ are the pressure and momentum fields. The speed of sound is specified by c, and the source term $q(t, \frac{x}{\varepsilon})$, $\varepsilon \ll 1$, is assumed to be slowly varying in time with small scale variations in space. This source term could simulate the release of latent heat from localized condensation, for example.

For traveling waves $(m,p)(t,x) = (m_0, p_0)\exp(i(\omega t - \kappa x))$, the dispersion relation of (1) is

$$\omega^2 - \kappa^2 c^2 = 0 \ . \tag{2}$$

Thus $\omega(\kappa) = \pm c\kappa$, so that in the continuous system all waves travel with the same velocity, $c = \pm\omega/\kappa$, without dispersion. Also, one can show, that the system preserves a global pseudo energy.

2 Implicit second-order staggered grid schemes

Before the new time integration scheme is introduced, we investigate two standard implicit second-order discretizations. These are the implicit trapezoidal rule and the BDF(2) scheme, which are commonly used in meteorological applications [3].

Their ability to compute reliable approximations to solutions of (1) is discussed with respect to the *discrete-dispersion relations* of these schemes (see [3, 9] for details).

Furthermore, the capability of the schemes to reproduce balanced modes is discussed. In the case of slow, short-wave forcing the balance is described by

$$c^2 m_x = q\left(t, \tfrac{x}{\varepsilon}\right) \quad \text{and} \quad p \equiv 0 \tag{3}$$

up to small perturbations introduced by the variation in time of the source term. The schemes should be able to essentially keep this balance. Furthermore, they should reproduce the balanced state in one time step by letting the step going to infinity.

Considering a semi-discretization in time, we leave the choice of a spatial discretization open for the moment. In the subsequent numerical experiments we choose a staggered grid with central differences for simplicity only.

Implicit trapezoidal rule. The implicit trapezoidal rule is derived by integrating the differential equation from t^n to t^{n+1}. The time integral on the right-hand side is then approximated by the trapezoidal quadrature rule. For the system of linear acoustics (1) this results into a Helmholtz problem for p^{n+1}, which is given by

$$p^{n+1} - \frac{c^2\Delta t^2}{4}\frac{\partial^2 p^{n+1}}{\partial x^2} = p^n - c^2\Delta t\frac{\partial m^n}{\partial x} + \frac{c^2\Delta t^2}{4}\frac{\partial^2 p^n}{\partial x^2} + \Delta t\, q^{n+1/2}\,. \tag{4}$$

The update for m is then obtained by

$$m^{n+1} = m^n - \frac{\Delta t}{2}\left(\frac{\partial p^n}{\partial x} + \frac{\partial p^{n+1}}{\partial x}\right)\,. \tag{5}$$

The method is symplectic and A-stable [4]. The discrete-dispersion relation results in a frequency-wave number relationship of the form

$$\omega_{\mathrm{r}} = \pm\frac{2}{\Delta t}\arctan\left(\mathrm{cfl}\cdot\sin\left(\frac{k\Delta x}{2}\right)\right) \tag{6}$$

where $\mathrm{cfl} = \frac{c\Delta t}{\Delta x}$ is the Courant–Friedrichs–Lewy (CFL) number, and the amplification factor per time step is given by $|A| \equiv 1$. Thus, essentially, the frequency ω_{r} depends not only on the wave number k, as in the continuous case, but it is also a function of the CFL number.

Figure 1 shows the discrete-dispersion relation for the trapezoidal rule (dashed line) applied to the linear acoustic equations for a CFL number $\mathrm{cfl} = 1$. The scheme slows down modes at almost all wave numbers, and this behavior is amplified the higher the wave number and the higher the CFL number are. Additionally, the trapezoidal rule is free of numerical dissipation. By letting $\Delta t \to \infty$, one obtains the relations

$$\frac{c^2}{2}\left(\frac{\partial m^n}{\partial x} + \frac{\partial m^{n+1}}{\partial x}\right) = q^{n+1/2} \quad \text{and} \quad \frac{\partial p^{n+1}}{\partial x} = -\frac{\partial p^n}{\partial x}\,. \tag{7}$$

This reflects the inability to reproduce balanced modes of the trapezoidal rule, and any perturbation of the system cannot dissipate.

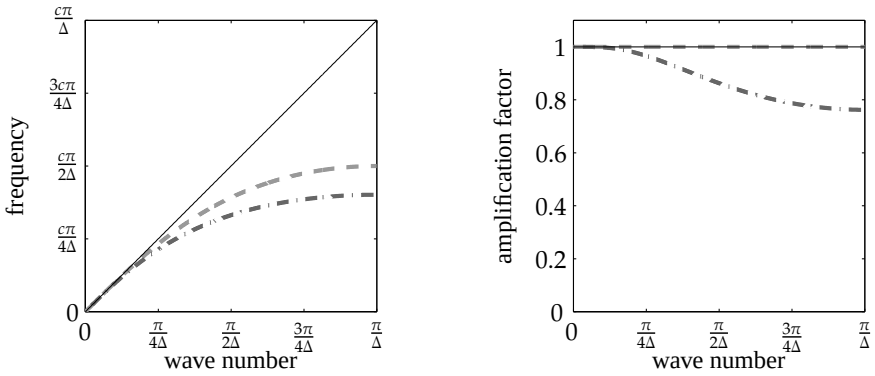

Fig. 1 Discrete-dispersion relations for the trapezoidal (dashed) and the BDF(2) rules (dot-dashed) applied to the linear acoustic equations using cfl = 1. Dispersion relation for continuous system is displayed as black line.

BDF(2) scheme. The BDF(2) scheme is a two-step method from the family of the so called *Backward Differentiation Formulas (BDF)*. Here, the left-hand side is approximated by the derivative of a parabola at t^{n+1}, which interpolates the solution at times t^{n-1}, t^n and t^{n+1}. For the acoustic system, this discretization results again in a Helmholtz problem for p^{n+1}, which is

$$p^{n+1} - \frac{4c^2\Delta t^2}{9}\frac{\partial^2 p^{n+1}}{\partial x^2} = \frac{4}{3}p^n - \frac{1}{3}p^{n-1} - c^2\Delta t\left(\frac{8}{9}\frac{\partial m^n}{\partial x} - \frac{2}{9}\frac{\partial m^{n-1}}{\partial x}\right) + \frac{2}{3}\Delta t\, q^{n+1} \,. \tag{8}$$

The update for m is obtained by

$$m^{n+1} = \frac{4}{3}m^n - \frac{1}{3}m^{n-1} - \frac{2}{3}\Delta t\frac{\partial p^{n+1}}{\partial x} \,. \tag{9}$$

The method is A- and L-stable [4].

The discrete-dispersion relation for the BDF(2) scheme is given again in Figure 1 (dot-dashed line). Concerning the phase error, it shows the same behavior as the trapezoidal rule, although it is considerably amplified. On the other hand, the scheme introduces dissipation for almost all modes. The damping is amplified for high wave and CFL numbers. In the limit $\Delta t \to \infty$ one obtains

$$c^2\frac{\partial m^{n+1}}{\partial x} = q^{n+1} \quad \text{and} \quad \frac{\partial p^{n+1}}{\partial x} = 0 \,,$$

and the scheme achieves balance in a single, sufficiently large, time step. This behavior is characteristic to backward differences formulas by construction [2].

This analysis reveals the dichotomy a practitioner is faced with when having to choose between the two time integrators: Either he could choose to minimize dispersion and preserve the amplitude of well resolved modes by using the trapezoidal

rule, or he could ensure that the solution rapidly relaxes to the balanced mode in case of short wave number forcing by the application of the BDF(2) scheme.

3 Multilevel method for long-wave linear acoustics

As described above, the ultimate goal is to filter out all acoustic short wave modes, which are not resolved in time, while sufficiently long wave data is integrated as accurate as possible. Here, we present a strategy for combining the two aspects into one single, scale-dependent numerical time integrator. It is exemplified by using the implicit trapezoidal rule and the BDF(2) scheme as base schemes. One could also use other time integrators (see [9] for a more general presentation), the only restriction is that they are linear in p^{n+1} and m^{n+1}.

Assume that we have scale dependent splittings of the pressure and momentum fields, i.e.

$$p = \sum_{\nu=0}^{\nu_m} p^{(\nu)} \quad \text{and} \quad m = \sum_{\nu=0}^{\nu_m} m^{(\nu)} \tag{10}$$

which could be a quasi-spectral or wavelet decomposition, splitting p and m into (local) high and low wave number components. The idea is to use for each scale component $(p^{(\nu)}, m^{(\nu)})$ a scale dependent blending of the two time integrators. Taking the μ-dependent convex combination with $\mu \in [0,1]$ of the two equations (4) and (8), and summing over the scales results in the Helmholtz problem

$$p^{n+1} - c^2\Delta t^2 \sum_{\nu=0}^{\nu_M} \left(\frac{\mu_\nu}{4} + \frac{4(1-\mu_\nu)}{9} \right) p_{xx}^{(\nu),n+1} = \sum_{\nu=0}^{\nu_M} \left(\mu_\nu \mathrm{R}_{\mathrm{TRA}}^{p,(\nu)} + (1-\mu_\nu)\mathrm{R}_{\mathrm{BDF2}}^{p,(\nu)} \right), \tag{11}$$

where

$$\begin{aligned} \mathrm{R}_{\mathrm{TRA}}^{p,(\nu)} &= p^{(\nu),n} - c^2\Delta t\, m_x^{(\nu),n} + \frac{c^2\Delta t^2}{4} p_{xx}^{(\nu),n} + \Delta t\, q^{(\nu),n+1/2}, \\ \mathrm{R}_{\mathrm{BDF2}}^{p,(\nu)} &= \frac{4}{3}p^{(\nu),n} - \frac{1}{3}p^{(\nu),n-1} - c^2\Delta t \left(\frac{8}{9}m_x^{(\nu),n} - \frac{2}{9}m_x^{(\nu),n-1} \right) + \frac{2}{3}\Delta t\, q^{(\nu),n+1}. \end{aligned} \tag{12}$$

The momentum update is derived from the blending of (5) and (9), which is

$$\begin{aligned} m^{n+1} = \sum_{\nu=0}^{\nu_M} \mu_\nu \left[m^{(\nu),n} - \frac{\Delta t}{2} \left(p_x^{(\nu),n} + p_x^{(\nu),n+1} \right) \right] + \\ (1-\mu_\nu) \left[\frac{4}{3}m^{(\nu),n} - \frac{1}{3}m^{(\nu),n-1} - \frac{2}{3}\Delta t\, p_x^{(\nu),n+1} \right]. \end{aligned} \tag{13}$$

The scale splitting is obtained by the application of restriction and prolongation operators used in standard multigrid algorithms. Let $\varphi = \sum \varphi^{(\nu)}$ be a grid function, which is decomposed into parts $\varphi^{(\nu)}$ living on the associated grid levels. Then, the

grid function on the coarsest level is obtained by the operation

$$\varphi^{(0)} = \left(R^{(0)} \circ R^{(1)} \circ \cdots \circ R^{(\nu_M - 1)} \right) \varphi \tag{14}$$

and the grid functions on finer levels are computed by

$$\varphi^{(\nu)} = \left(I - P^{(\nu-1)} \circ R^{(\nu-1)} \right) \circ \left(R^{(\nu)} \circ R^{(\nu+1)} \circ \cdots \circ R^{(\nu_M - 1)} \right) \varphi \, . \tag{15}$$

In our current approach the pressure is decomposed using the *full weighting* (restriction) and the *linear interpolation* (prolongation) operators [7]. They can be defined by their stencil, which are

$$R^{(\nu)} = \frac{1}{4} \begin{bmatrix} 1 & 2 & 1 \end{bmatrix} \quad \text{and} \quad P^{(\nu)} = \frac{1}{2} \begin{bmatrix} 1 & 2 & 1 \end{bmatrix} \, . \tag{16}$$

On a staggered grid the matching splitting in the momentum field is then defined by (for further details, see [9])

$$R^{(\nu)} = \frac{1}{8} \begin{bmatrix} 1 & 3 & 3 & 1 \end{bmatrix} \quad \text{and} \quad P^{(\nu)} = \begin{bmatrix} 1 & 1 \end{bmatrix} \, . \tag{17}$$

The description of the scheme is completed by the definition of the weighting function $\mu(\nu)$. In the subsequent tests, it is chosen such that the scheme in (11) and (13) associates the standard implicit trapezoidal scheme with all pressure modes corresponding to coarse grids with grid-CFL number $\mathrm{cfl} \leq 1$, while we nudge the discretization towards BDF(2) for pressure modes living on grids with $\mathrm{cfl} > 1$.

4 Numerical Results

Here, we shortly describe a test case with "multiscale" initial data in a periodic domain $x \in [0,1]$. Pressure and momentum fields are chosen in such a way that one obtains a right running acoustic simple wave with a sound speed of $c = 1$. The initial conditions are displayed in Figure 2 (top row). No source term is present (for further details see [9]). We use a grid with 512 cells (i.e. $\Delta x = 1/512$) and a CFL number $\mathrm{cfl} = 10$. The results are compared at a final time $t_{\mathrm{end}} = 3.0$, which is equivalent to 154 time steps. At this time the exact solution is identical to the initial data, and the wave has traveled three times across the domain.

The implicit trapezoidal rule produces the results in Figure 2 (bottom left). Here, and in the following, only pressure is displayed, since the momentum field is essentially the same. The results show what has already been revealed by the discrete-dispersion relation, i.e., the scheme achieves large-CFL stability by slowing down the short wave components of the solution. While the long-wave pulse has traveled at nearly correct speed, the short-wave oscillations have essentially stayed in place. Furthermore, their amplitude has not diminished.

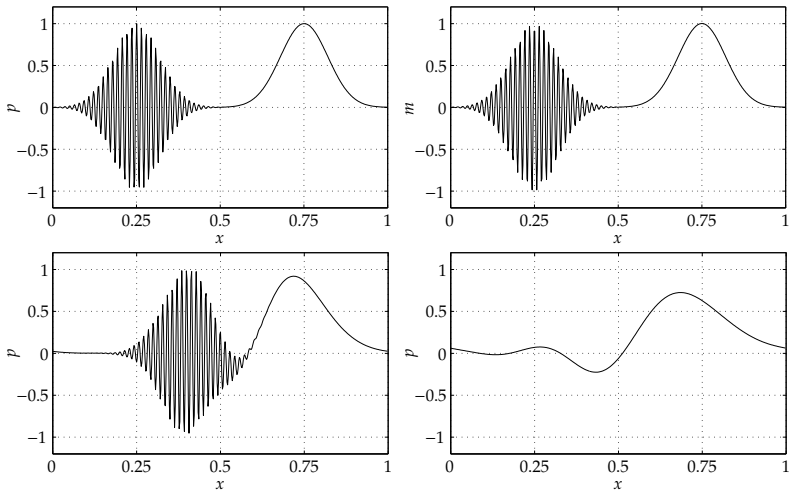

Fig. 2 Top row: "Multiscale" initial data. Bottom row: Numerical solution (pressure) with cfl $= 10$ at time $t_{\text{end}} = 3$ using the trapezoidal rule (left) and the BDF(2) scheme (right). Grid with 512 cells.

A different behavior is displayed by the BDF(2) scheme (Figure 2, bottom right). It has considerably more dispersion than the trapezoidal rule, and the damping of the scheme results in a smaller final amplitude, even for the long wave data. On the short scales, the diffusion is so high that at the final time this part of the solution has essentially vanished. Thus, the scheme is able to balance the short-wave modes that are not resolved in time, but it pays the price of simultaneously damping and dispersing the long scales.

The result of the simulation using the new blended scheme with five grid levels is displayed in Figure 3. For comparison, the result of the trapezoidal rule applied only to long wave data is also shown (dashed line). As one can see, the two results are nearly identical: The short wave data is filtered in such a way that only the long wave data is left after some time. On the other hand, the long wave data is integrated as well as one could hope when using a second-order method.

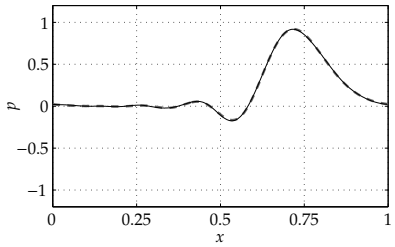

Fig. 3 Numerical solution (pressure) using the blended scheme on a grid with 512 cells and cfl $=$ 10 at time $t_{\text{end}} = 3$ (black line). For comparison, the result of trapezoidal rule obtained with only long wave initial data is plotted as gray dashed line.

5 Conclusion

The presented scheme effectively filters freely propagating compressible short-wave components, which cannot be accurately represented at long time steps. At the same time, dispersion and the amplitude errors for long-wave modes are minimized. Further tests show that in the presence of a source term, which slowly varies in time but has rapid spatial variations, solutions relax to an asymptotic balanced state (see [9]).

One of the next goals is to apply this scheme into a semi-implicit scheme for weakly compressible flows. The latter is an extension of a second-order projection method for incompressible flows as described in [8]. By using the trapezoidal rule in the implicit part of the scheme, one is faced with instabilities near shocks. This can partly be cured by so called off-centering. However, it also decreases the order of the scheme to one. The authors hope to obtain a second-order version by using the new scheme described in this note.

Acknowledgements R.K. thanks Piotr Smolarkiewicz for stimulating and challenging discussions on the theme of this paper. The authors thank Deutsche Forschungsgemeinschaft for its partial support of this work through grants KL 611/14 and KL 611/22 (MetStröm), and the Leibniz Association for partial support through its PAKT program.

References

[1] Davies, T., Staniforth, A., Wood, N., Thuburn, J.: Validity of anelastic and other equation sets as inferred from normal-mode analysis. Q. J. R. Meteorolog. Soc. **129**(593), 2761–2775 (2003)
[2] Deuflhard, P., Bornemann, F.: Scientific Computing with Ordinary Differential Equations, *Texts in Applied Mathematics*, vol. 42. Springer (2002)
[3] Durran, D.R.: Numerical Methods for Fluid Dynamics: With Applications to Geophysics, 2 edn. No. 32 in Texts in Applied Mathematics. Springer (2010)
[4] Hairer, E., Lubich, C., Wanner, G.: Geometric Numerical Integration: Structure-Preserving Algorithms for Ordinary Differential Equations. Springer (2006)
[5] Ohfuchi, W., Nakamura, H., Yoshioka, M., Enomoto, T., Takaya, K., Peng, X., Yamane, S., Nishimura, T., Kurihara, Y., Ninomiya, K.: 10-km mesh meso-scale resolving simulations of the global atmosphere on the Earth Simulator: Preliminary outcomes of AFES. J. Earth Simulator **1**, 8–34 (2004)
[6] Smolarkiewicz, P.K., Dörnbrack, A.: Conservative integrals of adiabatic Durran's equations. Int. J. Numer. Methods Fluids **56**(8), 1513–1519 (2008)
[7] Trottenberg, U., Oosterlee, C., Schüller, A.: Multigrid. Academic Press (2001)
[8] Vater, S., Klein, R.: Stability of a Cartesian grid projection method for zero Froude number shallow water flows. Numer. Math. **113**(1), 123–161 (2009)
[9] Vater, S., Klein, R., Knio, O.M.: A scale-selective multilevel method for long-wave linear acoustics. Acta Geophysica (2011). Submitted

The paper is in final form and no similar paper has been or is being submitted elsewhere.